THE JOURNAL OF PHYSICAL CHEMISTRY Letters

Letter

Cite This: J. Phys. Chem. Lett. 2018, 9, 1249−1253

pubs.acs.org/JPCL

Different Conformational Subensembles of the Intrinsically Disordered Protein α-Synuclein in Cells

Mohammad A. A. Fakhree, Ine Segers Nolten, Christian Blum, and Mireille M. A. E. Claessens*

Nanobiophysics Group, Faculty of Science and Technology, University of Twente, Enschede, The Netherlands

Supporting Information

ABSTRACT: The intrinsically disordered protein α-synuclein (αS) is thought to play an important role in cellular membrane processes. Although in vitro experiments indicate that this initially disordered protein obtains structure upon membrane binding, NMR and EPR studies in cells could not single out any conformational subensemble. Here we microinjected small amounts of αS, labeled with a Förster resonance energy transfer (FRET) pair, into SH-SY5Y cells to investigate conformational changes upon membrane binding. Our FRET studies show a clear conformational difference between αS in the cytosol and when bound to small vesicles. The identification of these different conformational subensembles inside cells resolves the apparent contradiction between in vitro and in vivo experiments and shows that at least two different conformational subensembles of αS exist in cells. The existence of conformational subensembles supports the idea that αS can obtain different functions which can possibly be dynamically addressed with changing intracellular physicochemical conditions.

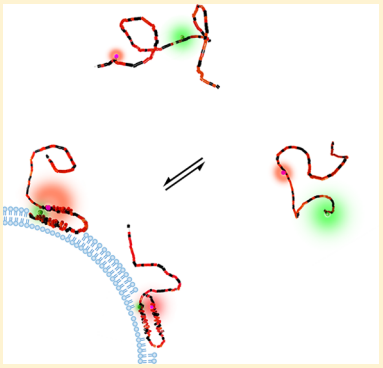

Alpha-synuclein (αS) is an intrinsically disordered protein (IDP) of 140 amino acids that is abundantly present in neurons. Its physiological functions are not well-understood, but it has been suggested to act as an interaction hub for different binding partners. Its aggregation is involved in the death of neurons in degenerative disorders such as Parkinson's disease and Lewy body dementia.

The term "intrinsically disordered" implies a lack of both secondary and tertiary structure. However, in solution, long-range contacts between residues cause αS to adopt an ensemble of significantly more compact structures.[1] In vitro experiments show that αS can organize into different folds that depend on binding partners.[2] αS has been reported to preferentially bind metal cations in the C-terminal region with residual structure[3] and to associate with several cytoplasmic proteins.[4−6] The best-characterized αS fold is the membrane-bound α-helical conformation.[7,8] αS binds anionic lipid bilayers and the membrane of small unilamelar vesicles of zwitterionic lipids in the liquid-ordered and gel phase.[9−11] Membrane binding is accompanied by folding of αS into α-helices that are oriented parallel to the membrane surface.[12−14] The membrane-bound conformation is thought to represent a functional fold of the protein (reviewed by Snead and Eliezer[15]). By inserting amphipathic α-helices into the membranes αS is thought to support curvature and (re)cluster vesicles.[16,17] Membrane-bound αS may additionally act as a nonclassical chaperone in SNARE-mediated fusion processes.[18]

However, in spite of the distinct conformations and conformational diversity of αS observed in vitro, NMR and EPR studies seem to indicate that in cells the disordered nature, observed for monomeric αS in solution, is preserved.[19,20] Considering the well-defined α-helical conformation of αS on membranes in in vitro experiments and the high number of αS molecules associated with cellular vesicles,[21] it seems unlikely that all of the αS proteins retain a disordered conformation inside cells. This controversy is a subject of intense discussion in the current literature, as reviewed by Pauwels et al.[22] Here we set out to resolve this contradiction and turned to imaging Förster resonance energy transfer (FRET) to discriminate distinctly different conformational ensembles inside cells.

In agreement with the literature on the subcellular distribution of αS in primary neurons that overexpress the protein, immuno-stained images of primary rat neurons show endogenous αS in two distinct localization patterns (Figure 1A,B).[23,24] Cytosolic endogenous αS is visible as a diffuse background while the membrane-bound form of the protein appears as distinct high-intensity puncta. To investigate possible differences of the protein conformation between the protein in the cytosol and the puncta we chose to microinject small amounts of fluorescently labeled αS into SH-SY5Y cells, a well-established neuronal cell model.[25] We observe the same αS distribution of puncta and diffuse background in cells injected with fluorescently labeled αS as in primary neurons (Figure 1C).

After we confirmed that the puncta in the images indeed represent αS on vesicles, using the method reported in ref 21 (Figure 2), an αS FRET probe designed to identify the membrane-bound α-helical conformation was introduced. In vitro experiments have shown that αS binds lipid vesicle membranes and micelles by organizing into an amphipathic α-helix.[10] This membrane-bound structure consists of two α-

Received: January 10, 2018
Accepted: February 23, 2018
Published: February 23, 2018

DOI: 10.1021/acs.jpclett.8b00092
J. Phys. Chem. Lett. 2018, 9, 1249−1253

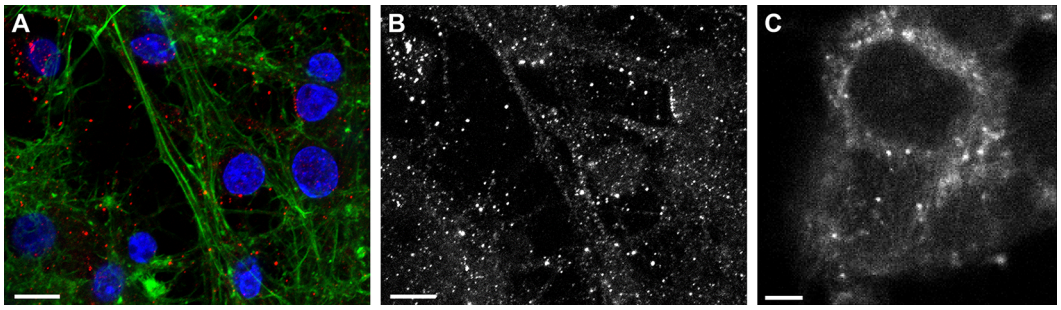

Figure 1. Localization of αS in cells. (A) Confocal microscopy image of rat primary neurons immuno-stained for αS (red), actin filaments (green), and nuclei (blue) (scale bar is 10 μm). (B) In the αS fluorescence from image A, here shown in a separate image, the presence of both a diffuse background fluorescence and distinct puncta is clearly visible. (C) Confocal microscopy image of a single SH-SY5Y cell that was microinjected with αS-AF488. The αS localization pattern is the same as that of primary neurons. The αS is visible as a diffuse background and distinct high-intensity puncta (scale bar is 5 μm).

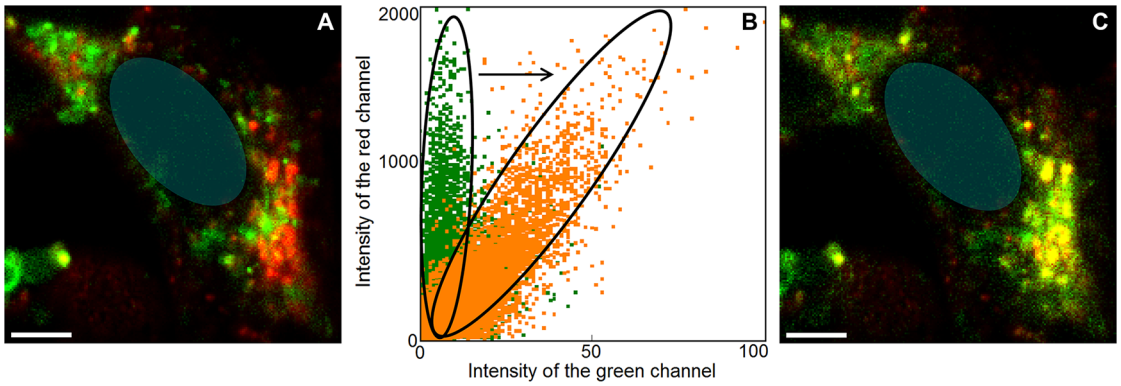

Figure 2. Membrane-bound αS. To confirm that the distinct puncta in the cells represent the vesicle-bound αS population, colocalization with the membrane marker WGA-AF647 was studied. (A) Confocal fluorescence image of SH-SY5Y cells microinjected with αS-AF488 (green) and stained with WGA-AF647 (red). Independent excitation and detection of the injected αS-AF488 (excitation 485 nm, detection 550/88 nm) and WGA-AF647 (excitation 640 nm, detection >665 nm) resulted in moderate colocalization. However, the two dyes form an efficient FRET pair, and this may render a fraction of the αS-AF488 invisible. (B) Scatter plots of the WGA-AF647 fluorescence intensity versus αS-AF488 fluorescence intensity. Photobleaching of WGA-AF647 dequenched the emission of αS-AF488, confirming the formation of a FRET pair and thus the nanometer proximity of the two dyes. The dequenching of the αS-AF488 fluorescence is visible as a shift of the intensity distribution. The original distribution presented in green changes upon bleaching to the distribution presented in orange. Data points were obtained per pixel. (C) Colocalization image obtained by combining the image of the initial WGA-AF647 fluorescence with the image of the αS-AF488 fluorescence after dequenching. Colocalization of αS-AF488 with the membrane is visible in yellow. In both images the position of the nucleus is indicated with a blue transparent oval; the scale bar is 5 μm.

helical segments comprising residues 3−37 and 45−92, joined by a flexible linker.[12,13,26,27] To discriminate between the membrane-bound α-helical and unstructured form of αS using changes in FRET efficiency, the distance between the labeled residues has to be markedly different in both forms. A maximum distance difference is achieved by labeling at amino acid positions 9 and 69 (Figure 3A). In the antiparallel α-helical form these residues are very close and thus show high FRET, while in the unstructured form the average distance between the residues is larger, resulting in lower FRET. Previous in vitro experiments confirmed the ability of this probe to discriminate between the membrane-bound and unstructured form of αS.[8]

Cells microinjected with αS, labeled with the AF488 FRET donor and AF568 FRET acceptor, show clear differences in FRET between different cellular structures or compartments (Figure 3B). In the composite image of the donor and acceptor emission intensity, low FRET is visible in green. With increasing FRET, the color in the composite image changes to yellow and red. The cytoplasm of the cells is visible in green, which represents low FRET; thus, the cytoplasm contains αS in unstructured from. In the cytoplasm, yellow and red puncta can be observed, originating from increased FRET. Clearly at least two distinctly different αS conformations are present in the cell. Because we[21] and others[28] confirmed that the puncta represent αS on small vesicles (Figure 2), we can even go one step further and conclude that the increased FRET in the puncta results from the membrane-bound α-helical conformation of αS.

For a more in-depth analysis, beyond single images, the FRET data has to be quantified. To quantify, the intensities in both the FRET donor (green) and acceptor (red) channel need to be related. However, the signal in both of these channels is a combination of the FRET signal and the cell's autofluorescence. The autofluorescence of the SH-SY5Y cells, with excitation at 485 nm, is not constant but varies both in and between cells. The ratio between the autofluorescence in the red and green channel, or autofluorescence index, is distributed as shown in the cumulative histogram (Figure 3D). The distribution of the autofluorescence index prevents the quantification of the data from the FRET images in terms of a FRET efficiency. Therefore, the data was collected in FRET index histograms for αS in the cytoplasm and on vesicles. The FRET index is given by the ratio of the acceptor emission intensity over the

DOI: 10.1021/acs.jpclett.8b00092
J. Phys. Chem. Lett. 2018, 9, 1249−1253

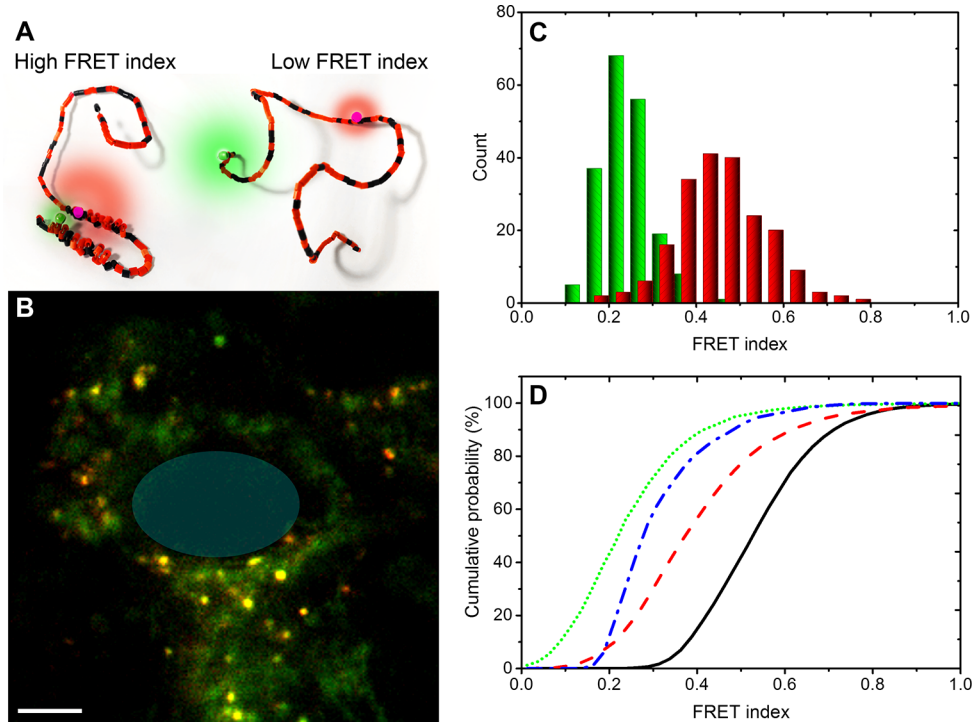

Figure 3. (A) Schematic of the antiparallel helices (left) and a representation of a disordered conformation of the FRET labeled αS. Differences in distance between the red and green emitting fluorophores give different FRET, here in the cartoon depicted by different relative sizes of the donor and acceptor emission halos. (B) Composite donor and acceptor fluorescence image of a single cell microinjected with the FRET-labeled αS. Regions of low FRET (green) and high FRET (yellow-red) can be discriminated. The position of the nucleus is indicated with a transparent blue oval (scale bar is 5 μm). (C) Histogram of the FRET index for αS in the cytoplasm (green) and on vesicles (red). (D) Cumulative probability histogram of the FRET index for αS in the cytoplasm (dotted green), on fibrils (dot-dashed blue), and on vesicles (dashed red). The autofluorescence index of unlabeled cells is indicated in solid black.

donor emission intensity. The FRET index will be low for low FRET and high for high FRET.

For both the membrane-bound αS and αS in the cytoplasm, the FRET index is distributed. For αS in the cytoplasm, the peak FRET index is found at 0.22 while for αS on vesicles a distinctly different peak FRET index of 0.45 is observed (Figure 3C). The shift to higher FRET indices for the vesicle-bound αS is even more clearly visible in the cumulative histogram (Figure 3D). The FRET index histogram of cytoplasmic αS is narrower than that of membrane-bound αS. This narrow distribution may be a result of compaction of the protein in the crowded environment of the cytoplasm as was observed in in-cell NMR experiments.[20] The broader FRET index distribution of vesicle-bound αS might be a result of the flexibility of the linker connecting the two α-helical regions of membrane-bound αS, resulting in a distribution of distances between the FRET pairs.[26,27,29] Additionally, in imaging small vesicles, below the optical resolution, the sampled volume will always also contain cytoplasm. This last factor together with the cellular autofluorescence index, partly overlapping with the FRET signal, prevents direct translation into a FRET efficiency. Hence these in vivo measurements cannot be directly compared with FRET studies on in vitro model systems. Control experiments in which a mixture of αS-AF488 and αS-568 was injected into the cells show that the observed high FRET on vesicles does not result from intermolecular FRET due to crowding of the labeled protein on the membrane surface or intermolecular interactions (Supporting Information, Figure S1).

To highlight the ability of our FRET probe to discriminate different αS conformations we included data on αS fibrils in the cumulative probability histogram (Figure 3D). The FRET index of the fibrils is rather narrow and peaks at 0.27. The different FRET index peak value and shape of the histogram indicate that a third conformational subensemble of the protein can be discriminated using these labeling positions and that the microinjected αS did not aggregate into amyloid fibrils in the cells.

In contrast to what has been previously reported, our data shows that the disordered nature of monomeric αS is not preserved in cells. In vivo NMR and EPR studies may have overlooked the membrane-bound conformation. The membrane-bound form of αS has been reported to be only a small fraction of the total αS in the brain.[30] The NMR study already indicated that it may not be possible to detect and discriminate lowly populated αS states with this bulk method.[20] In the NMR experiment, the αS concentration increases to tens of micromolars which may saturate membrane binding sites, resulting in an additional accumulation of unstructured αS in the cytoplasm. This excess of unstructured cytoplasmic αS may mask the presence of the membrane-bound population. The EPR studies were conducted on stage V/VI *Xenopus laevis* oocytes at even higher αS concentrations.[19] These cells are in an inactive state which does not require much membrane trafficking; trafficking vesicles will therefore be largely absent. The cytoplasm mainly contains yolk granules, and the absence of membrane-bound αS in these oocytes is therefore not surprising.

The sensitivity and ability to image and laterally resolve conformational differences makes our method very well-suited to single out conformational subensembles. Given the widely

DOI: 10.1021/acs.jpclett.8b00092
J. Phys. Chem. Lett. 2018, 9, 1249−1253

observed membrane-bound α-helical conformation in in vitro experiments, the existence of this conformational subensemble inside cells confirms our expectations. The used FRET probe was designed to identify the membrane-bound α-helical conformation of αS. Other probes can be designed to identify subpopulations representing αS bound to metal cations,[3] synaptobrevin,[18] 14-3-3,[31] actin,[5] and other proteins as reported in in vitro experiments. These multiple interactions may represent different conformational subensembles that coexist in a network of coupled binding equilibria. This distribution of αS over these different subensembles is probably tightly balanced. The sensitivity of these interactions to the changes in the intracellular conditions may make αS a hub in interaction networks.

■ ASSOCIATED CONTENT

Supporting Information

The Supporting Information is available free of charge on the ACS Publications website at DOI: 10.1021/acs.jpclett.8b00092.

Materials and methods (PDF)

■ AUTHOR INFORMATION

Corresponding Author

*E-mail: m.m.a.e.claessens@utwente.nl.

ORCID

Mohammad A. A. Fakhree: 0000-0002-8559-1377

Mireille M. A. E. Claessens: 0000-0002-2206-4422

Notes

The authors declare no competing financial interest.

■ ACKNOWLEDGMENTS

We thank Kirsten van Leijenhort-Groener and Irene Konings for assistance with experiments. We acknowledge Gerco Hassink for providing primary rat neurons.

■ REFERENCES

(1) Dedmon, M. M.; Lindorff-Larsen, K.; Christodoulou, J.; Vendruscolo, M.; Dobson, C. M. Mapping long-range interactions in alpha-synuclein using spin-label NMR and ensemble molecular dynamics simulations. *J. Am. Chem. Soc.* **2005**, *127*, 476−477.

(2) Uversky, V. N. A protein-chameleon: Conformational plasticity of alpha-synuclein, a disordered protein involved in neurodegenerative disorders. *J. Biomol. Struct. Dyn.* **2003**, *21*, 211−234.

(3) Binolfi, A.; Rasia, R. M.; Bertoncini, C. W.; Ceolin, M.; Zweckstetter, M.; Griesinger, C.; Jovin, T. M.; Fernandez, C. O. Interaction of alpha-synuclein with divalent metal ions reveals key differences: A link between structure, binding specificity and fibrillation enhancement. *J. Am. Chem. Soc.* **2006**, *128*, 9893−9901.

(4) Sousa, V. L.; Bellani, S.; Giannandrea, M.; Yousuf, M.; Valtorta, F.; Meldolesi, J.; Chieregatti, E. alpha-Synuclein and Its A30P Mutant Affect Actin Cytoskeletal Structure and Dynamics. *Mol. Biol. Cell* **2009**, *20*, 3725−3739.

(5) Esposito, A.; Dohm, C. P.; Kermer, P.; Bähr, M.; Wouters, F. S. alpha-synuclein and its disease-related mutants interact differentially with the microtubule protein tau and associate with the actin cytoskeleton. *Neurobiol. Dis.* **2007**, *26*, 521−531.

(6) Xu, J.; Kao, S. Y.; Lee, F. J. S.; Song, W. H.; Jin, L. W.; Yankner, B. A. Dopamine-dependent neurotoxicity of alpha-synuclein: A mechanism for selective neurodegeneration in Parkinson disease. *Nat. Med.* **2002**, *8*, 600−606.

(7) Ferreon, A. C. M.; Gambin, Y.; Lemke, E. A.; Deniz, A. A. Interplay of alpha-synuclein binding and conformational switching probed by single-molecule fluorescence. *Proc. Natl. Acad. Sci. U. S. A.* **2009**, *106*, 5645−5650.

(8) Veldhuis, G.; Segers-Nolten, I.; Ferlemann, E.; Subramaniam, V. Single-Molecule FRET Reveals Structural Heterogeneity of SDS-Bound alpha-Synuclein. *ChemBioChem* **2009**, *10*, 436−439.

(9) Nuscher, B.; Kamp, F.; Mehnert, T.; Odoy, S.; Haass, C.; Kahle, P. J.; Beyer, K. alpha-synuclein has a high affinity for packing defects in a bilayer membrane - A thermodynamics study. *J. Biol. Chem.* **2004**, *279*, 21966−21975.

(10) Pfefferkorn, C. M.; Jiang, Z. P.; Lee, J. C. Biophysics of alpha-synuclein membrane interactions. *Biochim. Biophys. Acta, Biomembr.* **2012**, *1818*, 162−171.

(11) Shvadchak, V. V.; Yushchenko, D. A.; Pievo, R.; Jovin, T. M. The mode of alpha-synuclein binding to membranes depends on lipid composition and lipid to protein ratio. *FEBS Lett.* **2011**, *585*, 3513−3519.

(12) Chandra, S.; Chen, X. C.; Rizo, J.; Jahn, R.; Südhof, T. C. A broken alpha-helix in folded alpha-synuclein. *J. Biol. Chem.* **2003**, *278*, 15313−15318.

(13) Jao, C. C.; Hegde, B. G.; Chen, J.; Haworth, I. S.; Langen, R. Structure of membrane-bound alpha-synuclein from site-directed spin labeling and computational refinement. *Proc. Natl. Acad. Sci. U. S. A.* **2008**, *105*, 19666−19671.

(14) Drescher, M.; Veldhuis, G.; van Rooijen, B. D.; Milikisyants, S.; Subramaniam, V.; Huber, M. Antiparallel arrangement of the helices of vesicle-bound alpha-synuclein. *J. Am. Chem. Soc.* **2008**, *130*, 7796−7797.

(15) Snead, D.; Eliezer, E. Alpha-synuclein function and dysfunction on cellular membranes. *Exp. Neurobiol.* **2014**, *23*, 292−313.

(16) Nemani, V. M.; Lu, W.; Berge, V.; Nakamura, K.; Onoa, B.; Lee, M. K.; Chaudhry, F. A.; Nicoll, R. A.; Edwards, R. H. Increased Expression of alpha-Synuclein Reduces Neurotransmitter Release by Inhibiting Synaptic Vesicle Reclustering after Endocytosis. *Neuron* **2010**, *65*, 66−79.

(17) Varkey, J.; Isas, J. M.; Mizuno, N.; Jensen, M. B.; Bhatia, V. K.; Jao, C. C.; Petrlova, J.; Voss, J. C.; Stamou, D. G.; Steven, A. C.; et al. Membrane Curvature Induction and Tubulation Are Common Features of Synucleins and Apolipoproteins. *J. Biol. Chem.* **2010**, *285*, 32486−32493.

(18) Burré, J.; Sharma, M.; Tsetsenis, T.; Buchman, V.; Etherton, M. R.; Südhof, T. C. α-Synuclein Promotes SNARE-Complex Assembly in Vivo and in Vitro. *Science* **2010**, *329*, 1663−1667.

(19) Cattani, J.; Subramaniam, V.; Drescher, M. Room-temperature in-cell EPR spectroscopy: alpha-Synuclein disease variants remain intrinsically disordered in the cell. *Phys. Chem. Chem. Phys.* **2017**, *19*, 18147−18151.

(20) Theillet, F. X.; Binolfi, A.; Bekei, B.; Martorana, A.; Rose, H. M.; Stuiver, M.; Verzini, S.; Lorenz, D.; van Rossum, M.; Goldfarb, D.; et al. Structural disorder of monomeric alpha-synuclein persists in mammalian cells. *Nature* **2016**, *530*, 45−50.

(21) Fakhree, M. A. A.; Zijlstra, N.; Raiss, C. C.; Siero, C. J.; Grabmayr, H.; Bausch, A. R.; Blum, C.; Claessens, M. The number of alpha-synuclein proteins per vesicle gives insights into its physiological function. *Sci. Rep.* **2016**, *6*, 30658.

(22) Pauwels, K.; Lebrun, P.; Tompa, P. To be disordered or not to be disordered: is that still a question for proteins in the cell? *Cell. Mol. Life Sci.* **2017**, *74*, 3185−3204.

(23) Boassa, D.; Berlanga, M. L.; Yang, M. A.; Terada, M.; Hu, J. R.; Bushong, E. A.; Hwang, M.; Masliah, E.; George, J. M.; Ellisman, M. H. Mapping the Subcellular Distribution of alpha-Synuclein in Neurons using Genetically Encoded Probes for Correlated Light and Electron Microscopy: Implications for Parkinson's Disease Pathogenesis. *J. Neurosci.* **2013**, *33*, 2605−2615.

(24) Spinelli, K. J.; Taylor, J. K.; Osterberg, V. R.; Churchill, M. J.; Pollock, E.; Moore, C.; Meshul, C. K.; Unni, V. K. Presynaptic Alpha-Synuclein Aggregation in a Mouse Model of Parkinson's Disease. *J. Neurosci.* **2014**, *34*, 2037−2050.

(25) Xicoy, H.; Wieringa, B.; Martens, G. J. M. The SH-SY5Y cell line in Parkinson's disease research: a systematic review. *Mol. Neurodegener.* **2017**, *12*, 10.

(26) Bussell, R.; Eliezer, D. A structural and functional role for 11-mer repeats in alpha-synuclein and other exchangeable lipid binding proteins. *J. Mol. Biol.* **2003**, *329*, 763−778.
(27) Lokappa, S. B.; Ulmer, T. S. alpha-Synuclein Populates Both Elongated and Broken Helix States on Small Unilamellar Vesicles. *J. Biol. Chem.* **2011**, *286*, 21450−21457.
(28) McLean, P. J.; Kawamata, H.; Ribich, S.; Hyman, B. T. Membrane association and protein conformation of alpha-synuclein in intact neurons - Effect of Parkinson's disease-linked mutations. *J. Biol. Chem.* **2000**, *275*, 8812−8816.
(29) Robotta, M.; Braun, P.; van Rooijen, B.; Subramaniam, V.; Huber, M.; Drescher, M. Direct Evidence of Coexisting Horseshoe and Extended Helix Conformations of Membrane-Bound Alpha-Synuclein. *ChemPhysChem* **2011**, *12*, 267−269.
(30) Lee, H. J.; Choi, C.; Lee, S. J. Membrane-bound alpha-synuclein has a high aggregation propensity and the ability to seed the aggregation of the cytosolic form. *J. Biol. Chem.* **2002**, *277*, 671−678.
(31) Perez, R. G.; Waymire, J. C.; Lin, E.; Liu, J. J.; Guo, F. L.; Zigmond, M. J. A role for alpha-synuclein in the regulation of dopamine biosynthesis. *J. Neurosci.* **2002**, *22*, 3090−3099.

DOI: 10.1021/acs.jpclett.8b00092
J. Phys. Chem. Lett. 2018, 9, 1249−1253